Corrections

PHYSIOLOGY

Correction for "Bone marrow stromal cells use TGF-β to suppress allergic responses in a mouse model of ragweed-induced asthma," by Krisztian Nemeth, Andrea Keane-Myers, Jared M. Brown, Dean D. Metcalfe, Jared D. Gorham, Victor G. Bundoc, Marcus G. Hodges, Ivett Jelinek, Satish Madala, Sarolta Karpati, and Eva Mezey, which appeared in issue 12, March 23, 2010, of *Proc Natl Acad Sci USA* (107:5652–5657; first published March 15, 2010; 10.1073/pnas.0910720107).

The authors note that the author name Jared D. Gorham should have appeared as James D. Gorham. Additionally, the author name Victor G. Bundoc should have appeared as Virgilio G. Bundoc. The corrected author line appears below. The online version has been corrected.

Krisztian Nemeth[a,b,1], Andrea Keane-Myers[c], Jared M. Brown[c], Dean D. Metcalfe[c], James D. Gorham[d], Virgilio G. Bundoc[c], Marcus G. Hodges[c], Ivett Jelinek[e], Satish Madala[c], Sarolta Karpati[b], and Eva Mezey[a,1]

www.pnas.org/cgi/doi/10.1073/pnas.1003664107

GENETICS

Correction for "BG1 has a major role in MHC-linked resistance to malignant lymphoma in the chicken," by Ronald M. Goto, Yujun Wang, Robert L. Taylor, Jr., Patricia S. Wakenell, Kazuyoshi Hosomichi, Takashi Shiina, Craig S. Blackmore, W. Elwood Briles, and Marcia M. Miller, which appeared in issue 39, September 29, 2009, of *Proc Natl Acad Sci USA* (106:16740–16745; first published September 11, 2009; 10.1073/pnas.0906776106).

The authors note the following statement should be added to the Acknowledgments: "This material is based on work supported in part by National Science Foundation Grant MCB-0524167."

www.pnas.org/cgi/doi/10.1073/pnas.1003235107

BIOCHEMISTRY

Correction for "Pathway of ATP utilization and duplex rRNA unwinding by the DEAD-box helicase, DbpA," by Arnon Henn, Wenxiang Cao, Nicholas Licciardello, Sara E. Heitkamp, David D. Hackney, and Enrique M. De La Cruz, which appeared in issue 9, March 2, 2010, of *Proc Natl Acad Sci USA* (107:4046–4050; first published February 16, 2010; 10.1073/pnas.0913081107).

The authors note that due to a printer's error, several of the Supporting Figures were referenced incorrectly in the main text. All references to Supporting Figure 3 should have instead referred to Supporting Figure 5, and all references to Supporting Figure 5 should have instead referred to Supporting Figure 3. All references to Supporting Figure 4 should have instead referred to Supporting Figure 6, and all references to Supporting Figure 6 should have instead referred to Supporting Figure 4. The online version has been corrected.

www.pnas.org/cgi/doi/10.1073/pnas.1003450107

BIOCHEMISTRY

Correction for "Remosomes: RSC generated non-mobilized particles with approximately 180 bp DNA loosely associated with the histone octamer," by Manu Shubhdarshan Shukla, Sajad Hussain Syed, Fabien Montel, Cendrine Faivre-Moskalenko, Jan Bednar, Andrew Travers, Dimitar Angelov, and Stefan Dimitrov, which appeared in issue 5, February 2, 2010, of *Proc Natl Acad Sci USA* (107:1936–1941; first published January 13, 2010; 10.1073/pnas.0904497107).

The authors note the following statement should be added to the Acknowledgments: "J.B. also acknowledges the support of Czech Grants LC535, MSM0021620806, and AV0Z50110509."

www.pnas.org/cgi/doi/10.1073/pnas.1003712107

Remosomes: RSC generated non-mobilized particles with approximately 180 bp DNA loosely associated with the histone octamer

Manu Shubhdarshan Shukla[a], Sajad Hussain Syed[a], Fabien Montel[b], Cendrine Faivre-Moskalenko[b], Jan Bednar[c,d], Andrew Travers[e], Dimitar Angelov[f,1], and Stefan Dimitrov[a,1]

[a]Université Joseph Fourier—Grenoble 1, Institut National de la Santé et de la Recherche Médicale, Institut Albert Bonniot, U823, Site Santé-BP 170, 38042 Grenoble Cedex 9, France; [b]Université de Lyon, Laboratoire de Physique (Centre National de la Recherche Scientifique, Unité Mixte de Recherche 5672) Ecole Normale Supérieure de Lyon, 46 Allée d'Italie, 69007 Lyon, France; [c]Centre National de la Recherche Scientifique, Laboratoire de Spectrometrie Physique, Unité Mixte de Recherche 5588, BP87, 140 Avenue de la Physique, 38402 Street Martin d'Heres Cedex, France; [d]Institute of Cellular Biology and Pathology, First Faculty of Medicine, Charles University in Prague and Department of Cell Biology, Institute of Physiology, Academy of Sciences of the Czech Republic, Albertov 4, 128 01 Prague 2, Czech Republic; [e]Medical Research Council Laboratory of Molecular Biology, Hills Road, Cambridge CB2 2QH, UK and Fondation Pierre-Gilles de Gennes pour la Recherche, c/o Laboratoire de Biotechnologie et Pharmacologie génétique Appliquée, École Normale Supérieure de Cachan, 61 Avenue de Président Wilson, 94235 Cachan Cedex, France; and [f]Université de Lyon, Laboratoire de Biologie Moléculaire de la Cellule, Centre National de la Recherche Scientifique, Unité Mixte de Recherche 5239/Institut National de la Recherche Agronomique 1237/Institut Fédératif de Recherche 128 Biosciences, Ecole Normale Supérieure de Lyon, 46 Allée d'Italie, 69007 Lyon, France.

Edited by Gary Felsenfeld, National Institutes of Health, Bethesda, MD, and approved November 25, 2009 (received for review April 29, 2009)

Chromatin remodelers are sophisticated nano-machines that are able to alter histone-DNA interactions and to mobilize nucleosomes. Neither the mechanism of their action nor the conformation of the remodeled nucleosomes are, however, yet well understood. We have studied the mechanism of Remodels Structure of Chromatin (RSC)-nucleosome mobilization by using high-resolution microscopy and biochemical techniques. Atomic force microscopy and electron cryomicroscopy (EC-M) analyses show that two types of products are generated during the RSC remodeling: (*i*) stable non-mobilized particles, termed remosomes that contain about 180 bp of DNA associated with the histone octamer and, (*ii*) mobilized particles located at the end of DNA. EC-M reveals that individual remosomes exhibit a distinct, variable, highly-irregular DNA trajectory. The use of the unique "one pot assays" for studying the accessibility of nucleosomal DNA towards restriction enzymes, DNase I footprinting and *ExoIII* mapping demonstrate that the histone-DNA interactions within the remosomes are strongly perturbed, particularly in the vicinity of the nucleosome dyad. The data suggest a two-step mechanism of RSC-nucleosome remodeling consisting of an initial formation of a remosome followed by mobilization. In agreement with this model, we show experimentally that the remosomes are intermediate products generated during the first step of the remodeling reaction that are further efficiently mobilized by RSC.

Intermediate | Mechanism | Nucleosome | Remodeling | Sliding

The fundamental unit of chromatin, the nucleosome, constitutes a barrier for several processes including transcription, repair, and replication. One of the main tools that the cell uses to overcome this barrier are the chromatin remodeling complexes. They possess the capacity to alter the histone-DNA-interactions (1) and to induce nucleosome mobilization (2). It has been also shown that the recently identified Swr1 remodeling complex possesses unique properties and is implicated in the exchange of the histone variant H2A.Z (3). Depending on the type of ATPase present, the remodeling complexes are classified into at least four distinct groups: the SWI2/SNF2, ISWI, CHD, and INO80 families (4).

The yeast RSC complex belongs to the SWI2/SNF2 family (5). It is abundant, essential for viability and comprises 15 subunits. RSC is involved in several processes, including transcriptional activation, DNA repair, and chromosome segregation (6). The structural analysis of RSC reveals the presence of a central cavity within the complex sufficient for binding a single nucleosome (7).

Much has been learned about nucleosome remodeling but, despite many efforts, neither the mechanism of the remodeling assembly action nor the organization of the remodeled nucleosomes are yet well understood. The SNF2 and ISWI families of remodelers exhibit some common activities: repositioning of nucleosomes in *cis*, generation of superhelical torsion, and DNA translocase activity (8–10). Activities specific to the SNF2 subfamily include ATPase stimulation by both DNA and nucleosomes and alteration of the DNase I digestion profile (1, 11). In contrast, the ATPase activity of the ISWI family of remodelers is only induced by nucleosomes and dependent on the N terminus of H4 and these remodelers appear to be involved in assembly of chromatin (12–14) The favored model, proposed for both SWI/SNF and ISW2 remodelers, requires a DNA loop formation on the nucleosome surface that further allows the sliding of the histone octamer (12, 15). This loop was proposed to be a prerequisite for the mobilization of the nucleosome (10).

In this work we have studied the mechanism of RSC-nucleosome mobilization by using high-resolution microscopy and biochemical techniques. We show that RSC uses an intriguing two-step mechanism for nucleosome remodeling. During the first step a stable non-mobilized particle, containing ~180 bp DNA associated loosely with the histone octamer, is generated. This particle, termed a "remosome," is then mobilized by RSC.

Results

RSC Generates Stable Non-Mobilized Nucleosome-Like Particles Associated With ~180 bp DNA. To study the mechanism of RSC-induced nucleosome remodeling we used centrally positioned nucleosomes reconstituted on a 255 bp fragment containing the 601 positioning sequence with 52 bp- and 56 bp-free DNA arms, respectively (Fig. S1). After incubation with RSC, the nucleosomes were visualized by atomic force microscopy (AFM) (Fig. S2). Fig. 1 shows a series of representative images for the nucleosomes incubated in the absence of RSC (*Control Sample*, *First Row*) or in the presence of RSC (*Second*, *Third*, and *Fourth Rows*). In the

Author contributions: M.S.S., S.H.S., F.M., C.F.-M., and J.B. performed research; M.S.S., C.F.-M., J.B., A.T., D.A., and S.D. analyzed data; A.T., D.A., and S.D. wrote the paper; and D.A. and S.D. designed research.

The authors declare no conflict of interest.

This article is a PNAS Direct Submission.

[1]To whom correspondence may be addressed: E-mail:stefan.dimitrov@ujf-grenoble.fr or Dimitar.Anguelov@ens-lyon.fr.

This article contains supporting information online at www.pnas.org/cgi/content/full/0904497107/DCSupplemental.

www.pnas.org/cgi/doi/10.1073/pnas.0904497107

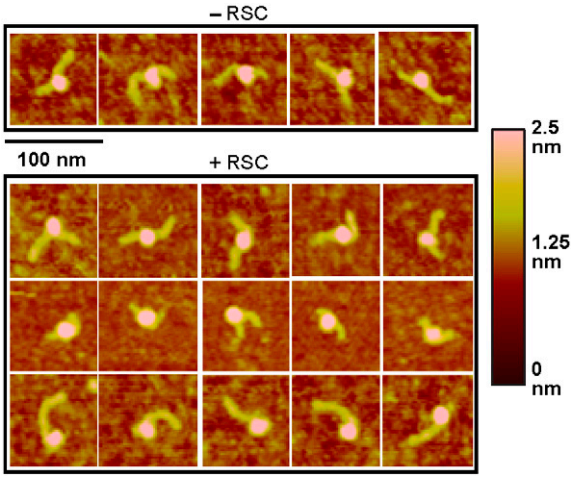

Fig. 1. AFM topography images of centrally positioned nucleosomes reconstituted on 255 bp 601 positioning sequence and incubated for 30 min with ATP in the absence of RSC (*1st Row*) or in the presence of RSC (*2nd*, *3rd*, and *4th Rows*).

Control Sample, the centrally positioned nucleosome core particle (*Pink Part* of the structure) is clearly distinguishable from the free DNA "arms" (*Yellow*). Upon incubation with RSC, three different groups of structures were observed. The organization of the first group (*Second Row*) is indistinguishable from the *Control Sample* (*First Row*). The second group (*Third Row*) exhibited shorter DNA arms than the *Control* and the *Third Group* consisted of completely slid nucleosomes with the histone octamer located at one end of the DNA (*Fourth Row*).

To understand how the different groups of particles were generated we performed remodeling reactions with two different amounts of RSC (30 and 60 fmols) and resolved the reaction mixtures on native PAGE (schematics in Fig. 2*A*) (Note that even the higher amount of RSC, used in the remodeling reaction, was at subsaturating concentration relative to the nucleosomes, that is, roughly 10 times less RSC than nucleosomes). The upper and the lower nucleosome bands were then excised from the gel, the nucleosomes were eluted and visualized by AFM (Fig. 2*B*–*E*). The *Control Sample* (incubated with ATP in the absence of RSC and consisting of a single upper band) contained, as expected, only centrally positioned nucleosomes (*Inset* of Fig. 2*B*). In contrast, the particles isolated from the upper band of the samples incubated with RSC were either identical to the controls or exhibited short free DNA arms (*Insets* in Fig. 2*C*). The frequency of nucleosomes with short arms dramatically increased when a higher amount of RSC was used in the remodeling reaction (Fig. 2*D*, *Inset*). The lower band contained mainly completely mobilized nucleosomes (*Inset* in Fig. 2*E*).

We next calculated the length of the DNA complexed with the histone octamer L_c ($L_c = L_{\mathrm{tot}} - L_+ - L_-$ where $L_{\mathrm{tot}} = 255$ bp and L_+ and L_- are the lengths of the longer and the shorter arm of the nucleosome measured from the AFM micrographs) and the position of the nucleosome relative to the center of DNA template $\Delta L = (L_+ - L_-)/2$ (16). The two-dimensional histogram $L_c/\Delta L$ for the control nucleosomes peaked at ~145 bp and ΔL is ~5–8 bp, which is in good agreement with the determination of the nucleosome position by biochemical approaches.

The two-dimensional histograms $L_c/\Delta L$ for the nucleosomes incubated with RSC and eluted from the gel slice were, however, quite different (Fig. 2*C*–*E*). Indeed, at the lower amount (30 fmol) of RSC present in the remodeling reaction, the $L_c/\Delta L$ map for the nucleosomes isolated from the upper electrophoretic band was broadened on the L_c axis indicating that particles associated with more DNA (>150 bp in length) were generated (Fig. 2*C*). The presence of the higher amount (60 fmol) of RSC resulted mainly in the generation of particles with short free DNA arms (isolated from the upper band) and containing ~180 bp DNA in complex with the histone octamer (Fig. 2*D*). Importantly, the nucleosome position ΔL relative to the DNA ends in these particles remained essentially the same as in the control particles, suggesting that the increased amount of DNA associated with the octamer is achieved through pumping of about 15–20 bp of DNA from each free DNA arm without nucleosome repositioning. For simplicity , in this text, we will call these particles *remosomes* (remodeled nucleosomes).

The $L_c/\Delta L$ map for the particles, eluted from the lower electrophoretic band of the RSC incubated samples, showed that both the complexed DNA length L_c and their position ΔL have altered and had average values of $L_c \sim 150$ bp and $\Delta L \sim 50$ bp. Thus, they represented a population of nucleosomes relocalized to the DNA end.

Remosomes are Ensemble of Distinct Structures with Different DNA Conformation. To study in more detail the organization of the RSC remodeling reaction products, we have next visualized them by Electron Cryo-Microscopy (EC-M). The EC-M pictures clearly show, as in the case of AFM images, the presence of three different types of structures (Fig. 3*A*), namely unperturbed centrally positioned nucleosomes (*First Row*), end-positioned nucleosomes (*Second Row*) and remosome-like structures (*Rows 3–6*). Typically, the remosomes exhibited shorter free DNA arms. The DNA conformation of each individual remosome was distinct, irregular and differed from the round shaped DNA conformation of the centrally positioned or slid end-positioned particles (Fig. 3 and Fig. S3). We conclude that the remosomes represent an ensemble of different nucleosome-like particles with distinct trajectories of an extended associated DNA. Note that in a typical RSC-nucleosome reaction mixture used for EC-M visualization about 20–25% of the particles exhibited remosome-like structure. In addition, the length of the EC-M measured remosomal DNA L_c was ~183 bp, while those of the unremodeled and slid nucleosomes were ~149 bp and ~143 bp, resp. (Table S3D). Importantly, the position of the remosome relative to the ends of DNA ($\Delta L/2$) did not change [$\Delta L/2$ for the parental (unremodeled) and the remosome were 3 bp and 6 bp, resp.] (see Table S3D). Therefore, by using two independent, high-precision microscopy techniques, we demonstrate that the remosome was not relocated but contained an additional ~30–35 bp of DNA associated with the histone octamer.

We have also studied the RSC remodeling of trinucleosomes, reconstituted on a DNA fragment, containing three 601 sequences. The presence of remosomes upon incubation with RSC was also observed (Fig. 3*C*). Because a single nucleosome can be converted into a remosome within the trinucleosomal array, this suggests that RSC is associated with a single nucleosome within the array and that it remodels only one nucleosome at the time. This indeed appeared to be the case (Fig. S4).

To test whether the described remosome structures could be generated not only on nucleosomes reconstituted with the "artificial" 601 DNA, we have analyzed the remodeling of nucleosomes reconstituted on a natural DNA fragment containing the 5S RNA gene of *Xenopus borealis* (Fig. 3*B*). As seen, upon incubation with RSC of these nucleosomes, the same types of remosome-like structures were visualized (Fig. 3*B*).

"In-Gel-One-Pot Assay" Shows Highly Perturbed Histone-DNA Interactions within the Remosome. To biochemically characterize the DNA path within the remosome at higher resolution, we have developed a unique approach termed "in-gel-one-pot assay" (see the schematics of the method in Fig. 4*A* and ref. 17). We used eight different ^{32}P-end labeled mutated 255 bp 601.2 DNA sequences to reconstitute centrally positioned nucleosomes, each

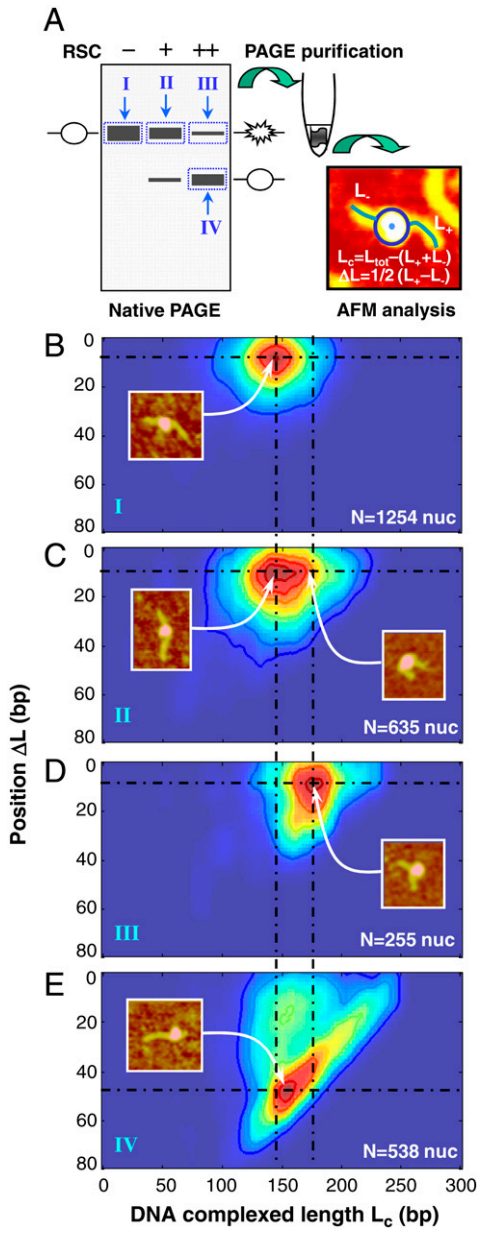

Fig. 2. The initial step of the RSC-nucleosome mobilization reaction is the generation of remosomes. (*A*) Schematics of the experiment. (*B*) Two-dimensional histogram $L_c/\Delta L$ representing the DNA complexed length L_c along with the nucleosome position ΔL (number of nucleosomes analyzed $N = 1254$ nucleosomes) for nucleosomes incubated in absence of RSC (*Control*) under the conditions described in (*A*) and gel eluted [*Fraction I*, see (*A*)]. (*C*) and (*D*), two-dimensional histograms for the upper gel band eluted nucleosomes incubated with 30 fmol [*Fraction II*, see (*A*] ($N = 635$) and 60 fmol [*Fraction III*, see (*A*)], ($N = 255$ nucleosomes) with RSC. (*E*) two-dimensional histogram for the nucleosomes eluted from the excised lower gel band after incubation for 30 mins with RSC ($N = 538$ nucleosomes). The inserts show the distinct nucleosome species corresponding to the different regions of the two-dimensional histograms. The color indicates the probability to find a nucleosome with the DNA complexed length L_c and the position ΔL. *Blue* corresponds to a low probability and *Red* to a high probability.

sequence bearing a unique *Hae*III restriction site, designated dyad-0 (d_0) to dyad-7 (d_7), where the number indicates the number of helical turns from the dyad. An equimolar mixture of the eight centrally positioned nucleosomes was incubated with RSC in the presence of ATP in a way to produce about 50% of slid nucleosomes and the reaction mixture was resolved on a 5% native PAGE (Fig. 4*A*). Then the upper band (containing the non-slid particles) was excised and digested in gel with increasing amount of *Hae*III under appropriate conditions. DNA fragments were isolated from the in-gel, *Hae*III-digested nucleosome particles and separated on 8% denaturing PAGE. The same experiment was carried out with control (incubated with RSC but in the absence of ATP) nucleosomes. After exposure of the dried gel, product bands from the experiment were quantified and expressed as percentage of cut fraction.

A typical experiment is presented in Fig. 4*B* and *C*. In the absence of ATP, the accessibility of dyad-7 to *Hae*III differed from the other *Hae*III sites. Indeed, even at low concentration (0.125 U/μl) of *Hae*III used, ~30% of dyad-7 was cleaved. Increasing the concentration of the restriction enzyme resulted in an increased dyad-7 cleavage that reaches ~70–75% at 8 U/μl *Hae*III. An apparent increase of the accessibility was also observed for dyad-6, which reached 20–25% cleavage at the highest concentration (8 U/μl) of *Hae*III. The cleavage at all the other sites was very low and remained largely unchanged at all concentrations of *Hae*III, suggesting a weak accessibility of these sites (Fig. 4*B* and *C*).

The picture was, however, completely different for the remosome fraction. In this latter case, the relative accessibility of dyad-7 sharply decreased (down to ~3-fold decrease at the highest concentration 8 U/μl *Hae*III). The relative accessibility of all the other sites (from dyad-5 to dyad-0) dramatically increased, the most pronounced increase (up to 10–15-fold in the different experiments) being observed at dyad-0. These data demonstrate that, within the RSC generated remosome, the DNA organization differed substantially from that of the unremodeled particle. The decreased accessibility at dyad-7 would reflect the RSC "pumping" of 15–20 bp-free linker DNA and the association of the sites around dyad-7 with the histone octamer and respective protection of these sites against *Hae*III digestion. The increased accessibility in the remosome of all the remaining dyads could be viewed as an evidence for strong perturbations in the histone-DNA interactions at these internally located sites within the remosome. Note that the efficiency of *Hae*III cleavage along the nucleosomal DNA was not completely uniform, but instead displayed a parabolic-like shape (Fig. 4*C*) with highest values at d_0 and d_7. Because within the native nucleosome the strongest histone-DNA interactions are found around d_0 (18), this shows that RSC has specifically altered these interactions and suggests that this alteration of the histone-DNA interactions around d_0 is important for further mobilization of the remosomes.

We have also carried out *Hae*III accessibility experiments on remosomes in solution (Fig. 4*D* and Fig. S5). In these experiments we used an equimolar mixture of 11 (bearing *Hae*III sites from d_0 to d_{10}), instead of 8 (as described above for the in-gel assay) nucleosomes. The nucleosome mixture was treated with RSC, as in Fig. 4*B*, and after separation on a native gel, the remosome fraction was eluted from the gel and digested with *Hae*III. As seen, the digestion profile, encompassing d_7 to d_0 was essentially the same as that of in-gel *Hae*III (Fig. 4, compare *C* with *D*). Therefore, the elution from the gel did not affect the structure of the particles. Remarkably, the accessibility of the *Hae*III sites (from d_7 to d_{10}) progressively increases, reaching a value very close to that of non-remodeled control particle at dyad-10 (Fig. 4*D* and Fig. S5). This suggested that the outermost *Hae*III site (d_{10}) was already weakly protected by histones, consistent with pumping of ~20 bp from the linker-DNA into the nucleosome. In addition, the time course of *Hae*III digestion shows a "jump" (an immediate cleavage) in the accessibility profile of the remosomes at the very first (*30 s*) time point of digestion for dyads d_0–d_5, this "jump" being highest at d_0 (Fig. S5), evidencing for the presence of loosely associated DNA within this region in the remosomes. These regions exhibited

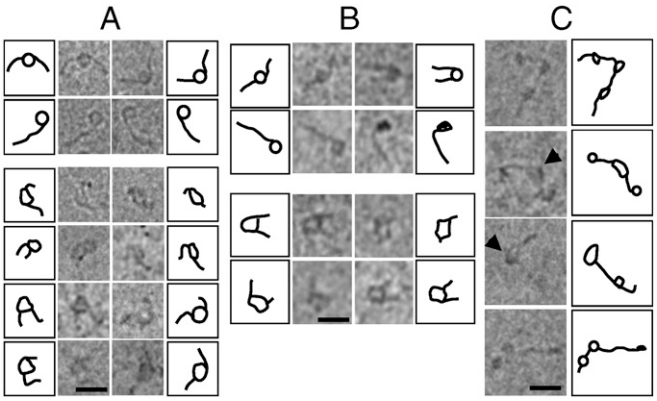

Fig. 3. EC-M visualization of remosomes. (*A*) Centrally positioned nucleosomes reconstituted on a 255 bp 601 DNA were treated with RSC, immediately vitrified, and visualized by EC-M. Each micrograph is accompanied by schematic drawing illustrating the shape of the DNA observed in the micrographs; bar, 25 nm. (*B*) Same as (*A*), but for nucleosomes reconstituted with a 255 bp DNA fragment containing the 5S somatic gene of *Xenopus borealis*; bar, 25 nm. (*C*) Same as (*A*), but for trinucleosomes reconstituted on a DNA fragment consisting of three 601 repeats; bar, 25 nm. The *First Row* illustrates the structure of a trinucleosome unaffected by RSC. The *Second* and the *Third Rows* show a typical structure of trinucleosome, containing a remosome (the *Black Arrowhead* indicates the centrally located remosome within the trinucleosome). Note the altered structure of the remosome compared to the end-positioned nucleosome in the trinucleosome. The *Fourth Row* shows a trinucleosome in which the centrally positioned nucleosome has been mobilized.

accessibility to *Hae*III only ~3-fold lower than that of naked DNA (not shown). Note that core particle treated with RSC showed a completely different *Hae*III digestion pattern compared to that of remosomes (Fig. S6), suggesting a distinct remodeled state.

Remosomes are Intermediate Structures Generated During the RSC-Nucleosome Mobilization Process. All the above data strongly suggest that the remosomes are intermediate structures generated by RSC that are further mobilized and converted completely into end-positioned nucleosomes. To confirm this, centrally positioned nucleosomes were incubated with RSC in presence of ATP for time points ranging from 0–64 min (Fig. 5*A*). After arresting the reaction they were submitted to partial DNase I digestion and run on PAGE under native conditions. Then the fractions containing the remosomes (Fig. 5*A*, the electrophoretic bands 1–8 with lower mobility) and two of the slid fractions (Fig. 5*A*, bands 9 and 10, obtained after 48 and 64 min of incubation with RSC, resp.) were excised from the gel, the DNA was eluted and run on a sequencing gel (Fig. 5*B*). Upon increasing the time of incubation with RSC, the accessibility of DNA within the remosome fractions was strongly altered (*Lanes 2–8*). In contrast, the digestion pattern of the control nucleosomes (incubated with RSC in the absence of ATP, *Lane 1*) became increasingly similar to that of naked DNA (*lane DNA*) and slid nucleosomes (*Lanes 9*, *10*). Because no mobilization of the histone octamer was observed in the remosome fraction (Fig. 2), we attributed the altered DNase I digestion pattern to reflect strong perturbations of the histone-DNA interactions within the remosome, a result in complete agreement with the data of in-gel-one-pot assay (Fig. 4). This conclusion is further confirmed by the Exo III mapping assay of the remosomes, which shows a completely different digestion pattern compared to those of both non-remodeled and slid particles (Fig. S7). The Exo III digestion of remosomes resulted in appearance of bands, predominantly, higher than 200 bp. This asymmetrical digestion pattern is completely compatible with the presence of overcomplexed DNA within the remosome (for detail, see legend of Fig. S7).

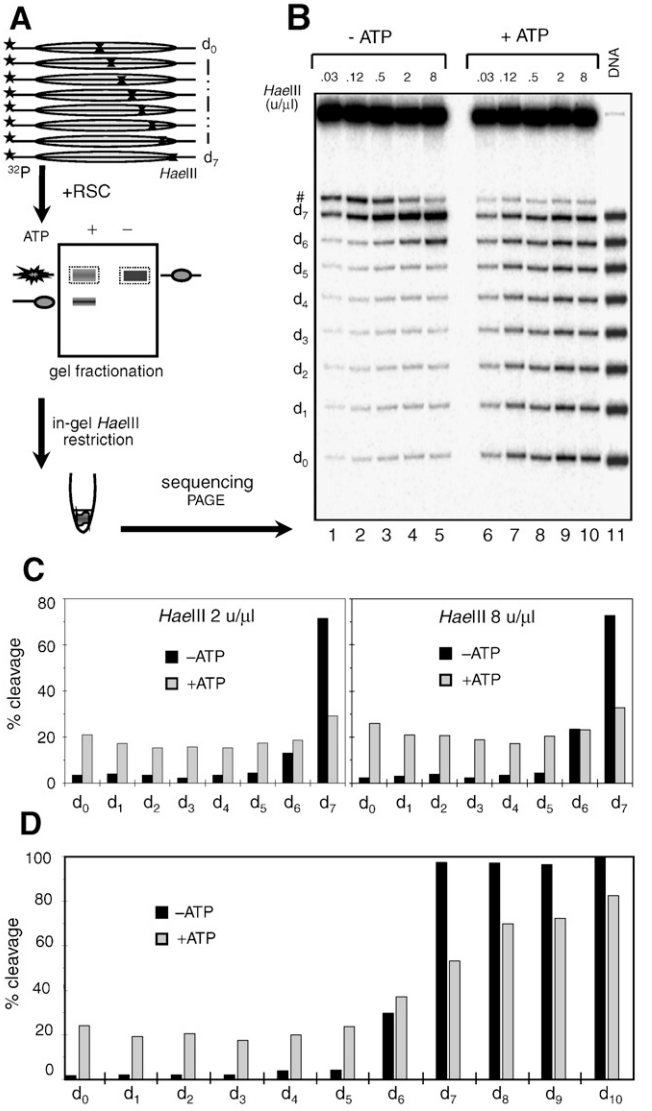

Fig. 4. In-gel and in-solution-one-pot restriction-accessibility assay of the RSC generated remosomes. (*A*) Schematics of the in-gel -one-pot assay. (*B*) *HaeIII* DNA digestion pattern of the non-slid nucleosomes incubated with RSC in the absence (*Left*) or presence (*right*) of ATP. The excised gel slices, containing the *Control* (incubated in the absence of ATP) or the non-mobilized (but treated with RSC in the presence of ATP) nucleosomes were incubated with the indicated units of *Hae*III, DNA was then isolated and run on denaturing PAGE. Lane 11, *Hae*III-digested naked DNA. The # indicates a fragment that corresponds to a *Hae*III site present only in "dyad 7" 601.2 fragment and located at 4 bp from the dyad 7 (d_7) site (*C*) Quantification of the data presented in (*B*). (*D*) *Hae*III accessibility of gel isolated remosomes in solution. An equimolar mixture of 11 centrally positioned nucleosomes (d_0 to d_{10}) were treated with RSC as in (*B*) and then run on a 5% PAGE. The bands corresponding to the *Control* (incubated with RSC in the absence of ATP) and the remosome fractions were excised from the gel and eluted. They were then digested with *Hae*III (2 U/μl) in solution and the cleaved DNA was run on an 8% denaturing PAGE. Quantification was carried out as in (*C*).

As the RSC remodeling reaction proceeds, the alterations in the DNase I patterns of the fractions containing the remosomes are characterized by the disappearance or decrease of intensity of some nucleosome-specific bands and the appearance (or increase of intensity) of some bands specific for naked DNA (Fig. 5*B*, see bands indicated by *Asterisks*). We have used this effect to measure the proportion of intact nucleosomes in the remosome fraction (*SI Text*). The proportion of the slid nucleosomes was directly

measured from the native PAGE (Fig. 5*A*). Because the total amount of all type of nucleosomes in the RSC reaction was known, this has allowed the calculation of the part of remosomes present in the reaction mixture (Fig. 5*C*). As seen during the remodeling reaction, the amount of intact nucleosomes rapidly decreases, whereas that of the slid nucleosomes increases but at a lower rate (Fig. 5*C*, compared to the initial slope of the *"Intact" Nucleosome Curve* with that of the *"Slid" Nucleosome Curve*). Consequently, during the remodeling reaction, the amount of remosomes initially increases, reaches a plateau, and then gradually decreases as the reaction proceeds (Fig. 5*C*). Importantly, when using our AFM data to measure the proportion of each individual particle species in the RSC reaction mixture, very similar curves were obtained (Fig. S8). Therefore, two completely independent techniques lead to the same conclusion. This demonstrates that the remosomes are intermediate products generated by RSC in an ATP-dependent manner, which are further converted into slid, end-positioned particles.

Remosomes are Bona Fide Substrates for Mobilization by RSC. If the remosomes are intermediates of the RSC-nucleosome mobilization reaction, they should be efficiently mobilized by RSC. We have addressed this question by using gel-purified remosome fractions. Briefly, we have incubated centrally positioned 601 nucleosomes with RSC for 16 and 48 min (under the same conditions as in Fig. 5), and after arresting the reaction we separated the different species on native PAGE (Fig. 6*A*). Then we excised the gel slices containing the remosome fractions (*R* and *R*+, obtained after 16 and 48 min of incubation, resp.), the slid nucleosomes (*S*), as well as the control fraction (*N*) (Fig. 6*A*). Note that under these conditions of incubation with RSC, both fractions (*R* and *R*+) contained mainly remosomes (Fig 5*C*). The particles from *R*, *R*+, *S*, and *N* fractions were eluted from the gel and a RSC-mobilization assay was carried out in the presence of ATP (Fig. 6*B*). As seen, the remosome fractions (*R* and *R*+) as well as the control nucleosomes (*N*) were efficiently mobilized by RSC, whereas the slid fraction, as expected, was not affected. In the absence of ATP, none of the different nucleosome species was mobilized (results not shown). We conclude that the remosomes are good substrates for RSC, and can be mobilized by the remodeler in an ATP-dependent manner.

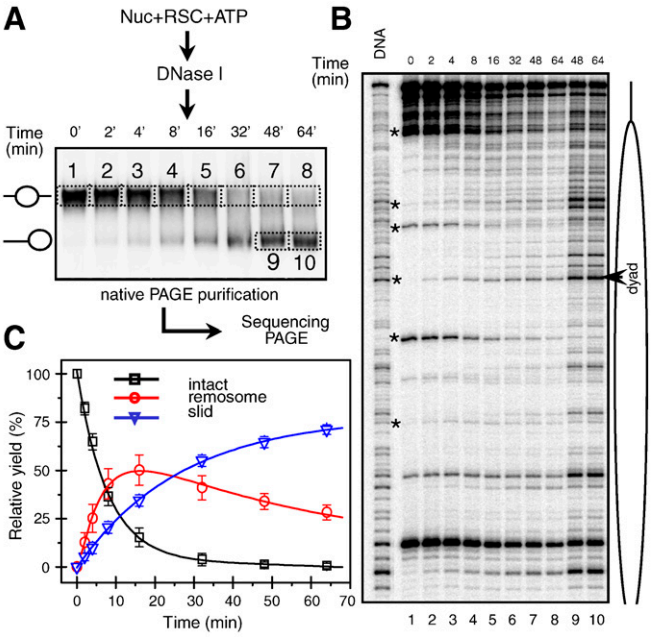

Fig. 5. The remosomes are intermediate structures generated during the RSC mobilization reaction. (*A*) Schematic presentation of the experiment. (*B*) 8% sequencing PAGE of the isolated DNA from the RSC remodeled and DNase I digested particles shown in (*A*). At the bottom of the gel, the numbers of the different fractions presented in (*A*) are indicated. At the top of the gel, the times of incubation with RSC are indicated. The last *Two Lanes* (48 and 64 min) show the DNase I digestion pattern of the gel purified mobilized particles (*A*). DNA, DNase I digestion profile of free 601 DNA. The position of the nucleosome is shown schematically on the *Right*; the *Arrow* shows the location of the nucleosome dyad. The bands, which change in intensity, are indicated by *Asterisks* and were used for calculation of the fraction of intact nucleosomes remaining in each remodeling reaction. (*C*) Normalized fractions of intact nucleosomes, remosomes, and slid nucleosomes (relative yields) determined from *A* and *B* versus the reaction time.

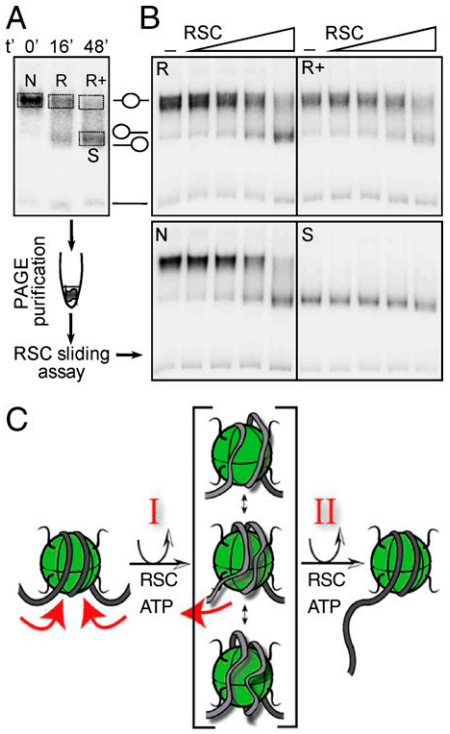

Fig. 6. The remosomes are bona fide substrates for RSC. (*A*) Description of the remosome mobilization experiment. (*B*) Mobilization of the gel eluted remosome fractions *R* and *R*+, the control nucleosomes (*N*) and the slid-end-positioned nucleosomes (*S*). Note that both remosome fractions, *R* and *R*+, in contrast to the end-positioned nucleosomes (*S*), are mobilized by RSC. (*C*) Schematic representation of the two steps, RSC-induced, nucleosome mobilization.

Discussion

In this work we have studied the mechanism of nucleosome mobilization by the remodeling factor RSC. Our results, in agreement with recently reported data (7), demonstrate that RSC is associated with a single nucleosome (Fig. S4) suggesting that it remodels only one nucleosome at the time. We show that, as a result of the remodeling reaction, two types of products were generated: nucleosome-like particles (remosomes) containing ~180 bp DNA and mobilized particles with the histone octamer located at either one of the DNA ends. RSC also has the capacity to generate remosomes in short, nucleosomal arrays. Remosomes are stable particles that can be separated from the slid end-positioned nucleosomes by PAGE under native conditions and eluted from the gel. Both free DNA arms of the remosomes are shorter compared to those of the non-remodeled particles and the position of the histone octamer relative to the center of the DNA fragment, remains identical to that of the non-remodeled structures. EC-M visualization demonstrated that the DNA wrapping around the histone octamer of the individual

remosomes was distinct but quite irregular, and importantly strongly differed from the helical projection of the DNA path of both the non-remodeled or slid end-positioned particles. The histone-DNA interactions within the remosome were strongly perturbed as shown by the unique in-solution- and in-gel-one-pot assays, DNase I footprinting, and Exo III mapping. These data, taken together, allow the conclusion that the remosomes do not exhibit a single, well-defined organization, but instead represent a multitude of structures, each structure exhibiting a distinct DNA trajectory around the associated histone octamer. The AFM visualization of the products of the remodeling reaction carried out at different concentrations of RSC strongly suggests that the remosomes are intermediate structures in the mobilization process that are subsequently converted into normal but end-positioned nucleosomes. This claim was supported by the experiments demonstrating the evolution of the different nucleosome species during the mobilization process and the capacity of RSC to efficiently mobilize the remosomes.

Based on our and previous data, we propose the following model for the mechanism of RSC-nucleosome remodeling (Fig. 6*C*). A single nucleosome associates with the RSC cavity (ref. 7 and Fig. S4). Upon ATP hydrolysis, RSC pumps on average 15–20 bp DNA from each one of the free DNA linkers without repositioning of the histone octamer (note that the pumping does not need to be simultaneous). This has two major consequences: (*i*) creation of a ~30–40 bp loop (or bulge) in the vicinity of the dyad and, thus, disruption of the strongest histone-DNA interaction within the nucleosome, and (*ii*) changes in the DNA path within the nucleosome. The particle created in this way can then dissociate from the remodeler. The loop is, however, unstable; it propagates and stops at different sites along the nucleosomal DNA where it partially spreads. Because the additional 15–20 bp DNA pumped from each linker is associated with the histone octamer (the in-gel- and in-solution-one-pot assay results), the loop, so generated, cannot dissipate. As a result, a multitude of stable structures with distinct, irregular DNA path are generated, that is, the remosome is formed. The observed structure of the remosome is consistent with a previous report demonstrating RSC-induced loss of constrained-DNA superhelicity (19). During the second step of the reaction, which requires the reassociation of the remosome and RSC and may require a conformational change in RSC, the remodeler functions as a true translocase by pumping and releasing DNA, as has been suggested for several remodelers in the past (9, 10, 12, 20).

The proposed model implies that DNA translocation occurs within the remosome, an inference that is in complete agreement with the experimental data showing that the remosomes are efficiently mobilized by RSC (Figs. 5 and 6). We speculate that the major in vivo function of RSC is the generation of remosomes. Because this process would minimize nucleosome collision, it would, in principle, facilitate several vital nuclear processes, including both DNA repair and transcription factor binding. We note that the observed organization of the remosome is quite consistent with the multiple facets of remodeler action, including alterations in DNase I digestion pattern (1), relocation of nucleosomes (2), generation of topological changes (21), and transfer of both H2A-H2B from nucleosomal substrate to H3-H4 tetrameric particle (22) as well as with the data obtained with single-molecule techniques (refs. 9, 10, and *SI Discussion*).

Materials and Methods

Plasmids, Preparation of DNA Fragments, Histone Purification, Nucleosome Reconstitution and Nucleosome Remodeling Reactions, DNase I Footprinting, Sliding Assay on Gel-Eluted Nucleosomes and Band Quantifications, In-Gel- and In-Solution-One-Pot Assays, and Exo III Mapping. Full information is provided in *SI Text*.

Atomic Force Microscopy, Image Analysis, and Construction of the Two-Dimensional Maps $L_c/\Delta L$. Nucleosome images were taken by using a Nanoscope III AFM (Digital Instruments™, Veeco). Several hundred of individual nucleosomes were analyzed per experiment by using a home-written Matlab (The Mathworks) script based on morphological tools (16). A detailed protocol is described in *SI*.

EC-M. Preparation of nucleosomes for EC-M was carried out as previously described (23). Images were taken on a Philips CM200 using Kodak SO 163 negative films or Philips Tecnai G2 Sphera microscope.

ACKNOWLEDGMENTS. We thank Dr. J. Workman for kindly providing us with the yeast strain expressing tagged RSC. This work was supported by grants from Institut National de la Santé et de la Recherche Médicale; Centre National de la Recherche Scientifique; the Association pour la Recherche sur le Cancer (Grant 4821); the Région Rhône-Alpes (Convention CIBLE 2008); and Agence Nationale de la Recherche: ANR-08-BLAN-0320-02 "EPIVAR" (to S.D.) and ANR-09-BLAN-NT09-485720 "CHROREMBER" (to D.A., S.D., and J.B). S.D. acknowledges La Ligue Nationale contre le Cancer (Equipe labellisée La Ligue). The research leading to these results has received funding from the European Community's Seventh Framework Programme FP7/2007-2013 under Grant agreement number 222008. J.B. acknowledges the support of the Grant Agency of the Czech Republic (Grant 304/05/2168). A.T. thanks l'Agence Nationale de Recherche for the award of a Chaire d'excellence.

1. Côté J, Peterson CL, Workman JL (1998) Perturbation of nucleosome core structure by the SWI/SNF complex persists after its detachement, enhancing subsequent transcription factor binding. *Proc Natl Acad Sci USA*, 95:4947–4952.
2. Langst G, Bonte EJ, Corona DF, Becker PB (1999) Nucleosome movement by CHRAC and ISWI without disruption or trans- displacement of the histone octamer. *Cell*, 97(7):843–852.
3. Mizuguchi G, et al. (2003) ATP-driven exchange of histone H2AZ variant catalyzed by SWR1 chromatin remodeling complex. *Science*, 303(5656):343–348.
4. Bao Y, Shen X (2007) SnapShot: chromatin remodeling complexes. *Cell*, 129(3):632.
5. Cairns BR, et al. (1996) RSC, an essential, abundant chromatin-remodeling complex. *Cell*, 87(7):1249–1260.
6. Gangaraju VK, Bartholomew B (2007) Mechanisms of ATP dependent chromatin remodeling. *Mutat Res*, 618(1-2):3–17.
7. Chaban Y, et al. (2008) Structure of a RSC-nucleosome complex and insights into chromatin remodeling. *Nat Struct Mol Biol*, 15(12):1272–1277.
8. Havas K, et al. (2000) Generation of superhelical torsion by ATP-dependent chromatin remodeling activities. *Cell*, 103(7):1133–1142.
9. Lia G, et al. (2006) Direct observation of DNA distortion by the RSC complex. *Mol Cell*, 21(3):417–425.
10. Zhang Y, et al. (2006) DNA translocation and loop formation mechanism of chromatin remodeling by SWI/SNF and RSC. *Mol Cell*, 24(4):559–568.
11. Kassabov SR, Zhang B, Persinger J, Bartholomew B (2003) SWI/SNF unwraps, slides, and rewraps the nucleosome. *Mol Cell*, 11(2):391–403.
12. Zofall M, Persinger J, Kassabov SR, Bartholomew B (2006) Chromatin remodeling by ISW2 and SWI/SNF requires DNA translocation inside the nucleosome. *Nat Struct Mol Biol*, 13(4):339–346.
13. Hamiche A, Kang JG, Dennis C, Xiao H, Wu C (2001) Histone tails modulate nucleosome mobility and regulate ATP-dependent nucleosome sliding by NURF. *P Natl Acad Sci USA*, 98(25):14316–14321.
14. Clapier CR, Langst G, Corona DF, Becker PB, Nightingale KP (2001) Critical role for the histone H4 N terminus in nucleosome remodeling by ISWI. *Mol Cell Biol*, 21(3):875–883.
15. Langst G, Becker PB (2001) ISWI induces nucleosome sliding on nicked DNA. *Mol Cell*, 8(5):1085–1092.
16. Montel F, Fontaine E, St-Jean P, Castelnovo M, Faivre-Moskalenko C (2007) Atomic force microscopy imaging of SWI/SNF action: mapping the nucleosome remodeling and sliding. *Biophys J*, 93(2):566–578.
17. Wu C, Travers A (2004) A 'one-pot' assay for the accessibility of DNA in a nucleosome core particle. *Nucleic Acids Res*, 32(15):e122.
18. Luger K, Mäder AW, Richmond RK, Sargent DF, Richmond TJ (1997) Crystal structure of the nucleosome core particle at 2.8 A resolution. *Nature*, 389:251–260.
19. Lorch Y, Zhang M, Kornberg RD (2001) RSC unravels the nucleosome. *Mol Cell*, 7(1):89–95.
20. Saha A, Wittmeyer J, Cairns BR (2005) Chromatin remodeling through directional DNA translocation from an internal nucleosomal site. *Nat Struct Mol Biol*, 12(9):747–755.
21. Kwon H, Imbalzano AN, Khavari PA, Kingston RE, Green MR (1994) Nucleosome disruption and enhancement of activator binding by a human SW1/SNF complex. *Nature*, 370(6489):477–481.
22. Bruno M, et al. (2003) Histone H2A/H2B dimer exchange by ATP-dependent chromatin remodeling activities. *Mol Cell*, 12(6):1599–1606.
23. Dubochet J, et al. (1988) Cryo-electron microscopy of vitrified specimens. *Q Rev Biophys*, 21(2):129–228.

Supporting Information

Shukla et al. 10.1073/pnas.0904497107

SI Text

SI Materials and Methods. ***Preparation of DNA fragments.*** The 255 bp 601 DNA probe used for reconstitution of centrally positioned nucleosomes was PCR amplified from pGEM-3Z-601 plasmid (kindly provided by J. Widom, Evanston, IL). 5′ end labeling was performed by using ^{32}P-labeled primer in PCR. For "in gel one pot restriction enzyme assay," a set of 8 or 11 pGEM-3Z-601.2 mutants were utilized, each containing *Hae*III site at a different superhelical location, as described before (1) (note that the "dyad 7" fragment contains an additional *Hae*III site located at 4 bp away from the d_7 site). Briefly, a 281 bp fragment was amplified using primers targeting the vector specific sequence flanking the 601.2 sequence. Labeling of the fragment was done as described above. The fragments were subsequently digested with *Sph*I to get a fragment of 255 bp with 57 and 51 bp linker DNA on left and right side, respectively. All the fragments were purified on 6% native acrylamide gel prior to use for nucleosome reconstitutions. Additionally, a 255 bp 5S DNA was PCR amplified from pXP-10 plasmid for electron cryomicroscopy experiments to visualize nucleosome remodeling reaction products.

Proteins and nucleosome reconstitutions. Recombinant *Xenopus laevis* full-length histone proteins were expressed in form of inclusion bodies in *E. coli* strain BL21(DE3) and purified as described (2). Remodels Structure of Chromatin (RSC) complex was purified essentially as described (3).

Nucleosome reconstitution was performed by the salt dialysis procedure (4, 5). For biochemical experiments requiring ^{32}P-end labeled DNA, 100 ng of ^{32}P-labeled 255 bp 601 or an equimolar mixture of the eight different ^{32}P-labeled 255 bp 601.2 mutated DNA fragments (100 ng) were added to the reconstitution mixture.

Nucleosome remodeling reaction. Typical remodeling reactions were performed with 150 fmol of nucleosomes and ≈15 fmol of RSC in remodeling buffer (RB) 10 mM Tris pH 7.4, 5% glycerol, 1 mM rATP, 2.5 mM $MgCl_2$, 1 mM DTT, 100μg/mL BSA, 50 mM NaCl, 0.01% NP40) in a volume of 7.5 μL at 29 °C. In scaled-up remodeling experiments, the nucleosome to RSC concentration ratio (≈10–20∶1) was maintained unless mentioned otherwise. Note that under our experimental conditions this nucleosome to remodeler ratio was sufficient to mobilize nucleosomes to saturation in 45 min.

DNase I footprinting assay. Three hundred femtomole of nucleosomes, reconstituted on ^{32}P-end-labeled 255 bp 601 DNA, were incubated with 30 fmol RSC in 15 μL RB for indicated time intervals. Reactions were stopped by addition of 0.02 units of apyrase and 2 μg of plasmid DNA. In the "zero time" control reaction, apyrase was added before addition of RSC. All the reactions were divided into two equal parts. In the first part, DNase I digestion was performed by addition of 0.5 units of DNase I. EDTA was added to 25 mM to stop DNase I cleavage. Both the undigested and DNase I digested samples were resolved in parallel on separate native polyacrylamide gels (29∶1) in 0.25X Tris Borate EDTA at room temperature. The native gel corresponding to the undigested sample was used to quantify nucleosome sliding. From the second gel, for resolving DNase I digested samples, bands corresponding unmobilized and mobilized nucleosomes were excised. DNA was eluted, filtered, deproteinized by phenol∶chloroform treatment, precipitated, and run on 8% denaturing PAGE.

Gel band quantifications. The gel bands (Fig. 5) were quantified by integration of rectangles using the Multigauge v3.0 (Fuji) software. In the case of Fig. 5*A*, the fraction of mobilized nucleosomes (S) was determined by dividing the signal of the fast migrating band to the total radioactivity, i.e., to the sum of the signals of the slow and fast migrating bands.

The quantification of the fraction of native nucleosomes (N) present at each studied time point of the remodeling reaction (Fig. 5*C*) was based on the observation that upon generation of remosomes some typical nucleosomal bands disappear, while other typical naked DNA bands in the DNase I digestion profile appear concomitantly (Fig. 5*B*; see bands marked with asterisks). Therefore, the relative intensity of these bands is a measure of the amount of intact nucleosomes in the remodeling reaction at the respective time point. The signals of these bands for each time point of RSC remodeling, normalized to the sum of the signals of all bands (the total radioactivity in the lane) were determined by integration. These values were further normalized assuming 100% and 0% intact nucleosomes at the time points $t = 0$ and $t = 64$ min, respectively. This assumption is based on the observation of a full saturation at 48 and 64 min of the dependencies of the intensity of each band versus time of RSC remodeling (data not shown, but see Fig. 5*C*, "intact nucleosomes"). Finally, values for different bands in each line were averaged and then multiplied to the corresponding fractions $N + R = 1 - S$ (determined from Fig. 5*A*; see above). This allows the determination of the fraction of intact nucleosomes (N) present at the given time point of the remodeling reaction. The fractions of remosomes R at each time point were calculated as $R = 1 - N - S$.

Sliding assay on gel eluted nucleosomes. Centrally positioned 150 fmol 601 nucleosomes were incubated with RSC in the remodeling reaction as described above. The reaction was stopped at 16 and 48 min by addition of 0.01 units of apyrase and 1 μg of plasmid DNA, because under these conditions the nonmobilized fraction contains essentially remodeled nucleosome particles. Reaction products were resolved on 5% native polyacrylamide gel. Bands, corresponding to unmobilized fractions from 0, 16, and 48 min, and mobilized fraction from 48 min reaction time points were excised. Excised bands were then cut in small pieces and soaked in 80 μL elution buffer containing 10 mM Tris pH 7.4, 0.25 mM EDTA, and 10 mM NaCl, at 4 °C for 3 h with gentle shaking. Cold 601 255 bp nucleosomes (0.75 pmol) were added in the elution buffer to maintain the stability of eluted nucleosomes. Eluted nucleosomes were filtered through glass fiber filter under low-speed centrifugation ($200 \times g$) to remove acrylamide particles, washed and concentrated using 100 kDa cutoff spin filters. Eluted nucleosomes, divided into equal aliquots, were further subjected to next round of sliding reaction in the standard remodeling conditions, as described above, for 45 min with increasing amount of RSC (in twofold increments) with the maximum being 15 fmol.

In gel one pot assay. The remodeling reaction was performed in a five times scaled-up reaction with nucleosomes reconstituted using an equimolar mixture of the eight 601.2 mutants. Nucleosomes [0.75 pmol (Control reactions with no ATP) or 1.50 pmol (remodeling reactions)] were incubated with the amount of RSC (35 fmol for control and 70 fmol for remodeling reaction, respectively) sufficient to mobilize 45–60% of the nucleosomes. Reactions were stopped by adding 0.05 units of apyrase. Prior to loading on 5% native polyacrylamide gel, 6.25 pmol of cold

255 bp 601 middle positioned nucleosomes were added to each reaction as a carrier in order to maintain stability during subsequent procedures. Both control and remodeling reaction were equally divided in five aliquots and resolved on 5% native polyacrylamide gel. Bands corresponding to control unremodeled and unmobilized remodeled nucleosomes were excised, collected in siliconized eppendorf tubes, crushed very gently, and immersed with 50 μL restriction buffer (10 mM Tris pH 7.4, 10 mM $MgCl_2$, 50 mM NaCl, 1 mM DTT, and 100 μg/mL BSA) containing increasing amount of *Hae*III (0.03, 0.12, 0.50, 2.0, 8 units/μL) for 5 min at 29 °C. The reaction was stopped by addition of an equal volume (50 μL) of stop buffer containing 0.2% SDS and 40 mM EDTA. DNA was eluted from the gel slices, purified as described above, and run on 8% denaturing gel. The quantification of extent of accessibility at different superhelical locations in the nucleosome was performed using Multigauge Software (Fuji). For in-solution restriction analysis, nucleosomes were reconstituted on an equimolar mixture of 11 601.2 fragments. Nucleosomes were remodeled under the same conditions as described above, resolved on 5% native gel, and fractions corresponding to control or remosome fractions were eluted and digested with *Hae*III (2 U/μL) for indicated time points. DNA was extracted, resolved, and quantified as described above.

Gel purification of nucleosomes for Atomic Force Microscopy analysis. Six hundred femtomoles of the 255 bp 601 nucleosomes were incubated with increasing amount of RSC (30 and 60 fmol, respectively) in the remodeling reaction as described above for 30 min. However, the final reaction volumes in this experiment were adjusted to 10 μL to be convenient for loading the samples on gel. After stopping the reaction with apyrase, reaction products were resolved on 5% native polyacrylamide gel. To ascertain the migration of unmobilized and mobilized species, a replicate of the experimental set containing ^{32}P-labeled 601-255 bp nucleosomes was done and run on the same gel. Nucleosomes were eluted from excised bands, corresponding to control, remodeled, and slid species, as described before. Eluted nucleosomes were filtered through glass fiber filter, prior to sample preparation for AFM analysis.

Exo III mapping of nucleosomes. Centrally positioned nucleosomes were reconstituted on a 5′ ^{32}P-labeled 255 bp 601 DNA sequence and remodeled with RSC in the conditions to generate ≈50% of slid species. Nucleosome fractions corresponding to unremodeled, remosome, and slid fractions were eluted from the native gels as described above, digested with Exo III for indicated time points, and analyzed on an 8% denaturing gel.

Atomic Force microscopy, image analysis, and construction of the 2D maps $L_c/\Delta L$. For the AFM imaging, the nucleosomes were immobilized onto APTES-mica surfaces (Aminopropyltriethoxysilane) as described previously (6). To automatically analyze AFM images, we have written a Matlab (The Mathworks) script based on morphological tools. Using this script, we are able to isolate single mononucleosomes from other objects present on the image (for example, surface roughness, naked DNA, two connected nucleosomes).

To remove the piezoelectric scanner thermal drift, flattening of the image is performed. The use of a height criterion ($h > 0.5$ nm where h is the height of the object) eliminates interference from the shadow artifact induced by high objects on the image. Then we select nucleosomes based on area criteria and height thresholding. Using a hysteresis height thresholding, we verify the presence of an Nucleosome core particle (NCP) on each selected objects. For each mononucleosome, the NCP center of mass is localized and an Euclidian distance map can be calculated from this origin. After exclusion of the NCP part, the skeletons of the free arm regions are obtained by thinning. By applying the previous distance map, the length of each arm is measured from the NCP centroid. The longest arm is named L_+ and the shortest L_-. DNA complexed length is deduced by $L_c = L_{\text{tot}} - L_- - L_+$ where L_{tot} is 255 bp in this case. The position of the nucleosome relatively to the DNA template center is calculated as $\Delta L = (L_+ - L_-)/2$. It is important to notice that the position defined in this way corresponds to the location of the most deeply buried base pair, which might differ from dyad axis position (strictly defined for symmetric nucleosomes).

As the length of each nucleosome arm (L_+ and L_-) is measured from the centroid of the NCP, it is necessary to subtract the crystallographic radius (5.5 nm) of the NCP to get the actual arm length.

To construct the 2D histogram, a 10 bp-sliding box is used. For each coordinate $(\Delta L_0, L_{c0})$ in $[0, 150\text{ bp}] \times [0, 300\text{ bp}]$, nucleosomes with a DNA complexed length included in the range $[L_{c0} - 5\text{ bp}, L_{c0} + 5\text{ bp}]$ and a position included in the range $[\Delta L_0 - 5\text{ bp}, \Delta L_0 + 5\text{ bp}]$ are counted. After normalization, a smooth distribution is obtained that represents mathematically the convolution of the real experimental 2D distribution with an 8 bp square rectangular pulse.

During the AFM mobilization assays, we have observed nucleosomes where only one DNA arm is visible. The single DNA arm exhibits the same length as one arm of the overcomplexed two-arm nucleosome, and is also clearly different from the slid end-positioned one-arm nucleosome. Electron cryomicroscopy (EC-M) experiments do not show any of such overcomplexed one-arm nucleosome. These types of objects most probably result from the interaction with the functionalized mica surface during the deposition process that might perturb the more labile structure of the "remosomes." This type of "false one-arm" nucleosome is very rarely observed on control nucleosomes (−RSC). Accordingly, those objects were discarded during the analysis.

Electron Cryomicroscopy. Samples for electron cryomicroscopy were prepared as described previously (7). The electron microscopy grids covered with perforated support film were used. The film surface was treated by subsequent evaporation of carbon and carbon–platinum layers and the plastic support was dissolved prior to use. Three microliters of solution were deposited on the grid held in the tweezers mounted in the plunger. The majority of the liquid was blotted away with Whatman No. 4 blotting paper and the grid immediately plunged into liquid ethane held at −183 °C. The specimen was transferred without rewarming into the electron microscope using Gatan 626 cryotransfer holder. Images were acquired at 80 kV accelerating voltage either on Philips CM200 using Kodak SO 163 negative films, 66000x direct magnification, and 1.5 μm underfocus or Philips Tecnai G2 Sphera microscope equipped with Ultrascan 1000 CCD camera (Gatan) using 14500x direct microscope magnification (0.7 nm final pixel size) and 2.5 μm underfocus. Negatives were developed for 12 min in full-strength Kodak D19 developer.

SI Discussion. We have proposed a two-step model for the RSC-induced nucleosome mobilization (Fig. 6). According to the model, upon ATP hydrolysis during the first step, RSC pumps on average 15–20 bp DNA from each linker DNA without nucleosome relocation. This leads to the disruption of histone DNA contacts, formation of a loop on the nucleosome surface, and thus, generation of the remosome. RSC then dissociates from the remosome. During the second step, RSC reassociates with the remosome and functions as a unidirectional translocase by pumping and releasing DNA, as has been suggested for a number of remodelers (8–11). Note that our model differs from the proposed ones because it consists of two distinct steps and, during the first one, RSC pumps DNA from both linkers. The question arises if the model is consistent with the available data and, in

particular, with the data from single molecule experiments and the existence of a single translocase domain in RSC.

Single molecule experiments demonstrate that RSC is able to generate a loop through its translocase domain on both naked DNA and nucleosome in an ATP-dependent manner. Importantly, the direction of translocation can change (10, 11), but how RSC achieves this is unclear from microscopic point of view. A change of the direction of translocation may involve either flipping of the nucleosome inside the remodeler without its dissociation (or partial transient dissociation) or conformational transition of the remodeler (discussed in ref. 12). Note that in our model the pumping of the individual linkers is ATP- and RSC-dependent but it does not have to be simultaneous to generate the metastable state containing more DNA (the remosome). Consequently, the single translocase domain of RSC would be able to achieve the bidirectional linker DNA pumping.

Our data demonstrate that the remosome contains on average ≈30–40 bp of overcomplexed DNA, suggesting that at least a bulge (or loop) of this size should be generated during the action of RSC. Single molecule experiments in real time evidenced for the formation of mostly larger loops using as a substrate either a nucleosome (up to 1,200 bp, with an average ≈110 bp, see ref. 11) or DNA alone (10). What is the origin of this difference? For the moment, it is difficult to give a precise answer to this question. We would like, however, to stress that the single molecule experiments using optical (or magnetic) tweezers enable to observe RSC action during DNA pumping in real time on the nucleosome (or on naked DNA) whereas by single molecule AFM or electron cryomicroscopy visualization, metastable nucleosomal states after the action (and the release) of RSC are analyzed. Therefore, these two kinds of single molecule experiments (namely AFM and electron cryomicroscopy on one hand and optical tweezers on the other) cannot be compared directly, but give complementary information. We also note that the single molecule experiments with nucleosomal DNA templates were performed using an extension regime of 3–6 pN (10). It cannot be excluded that such forces could alter any partition of the force exerted by the remodeler.

We would also like to note that the remosome is a metastable intermediate, relative to the fully remodeled nucleosome. The particular organization of the remosome, the presence of the bulge, and the perturbed histone-DNA interactions within it, is quite compatible with the described consequences of the action on RSC on the nucleosome, including generation of topological changes (13), higher accessibility to DNase I (14), and restriction enzymes and the transfer of H2A-H2B from nucleosomal substrate to H3-H4 tetrameric particle (15).

The RSC-induced nucleosome remodeling has been the object of several studies, but no data have been reported on the identification of a remosome particle. However, the vast majority of the reported experiments in the literature were designed to describe the initial and final state of the nucleosome after remodeling reaction. To our knowledge, no biochemical assays were applied to isolate and study the "preslid" structure of the nucleosome in the presence of the remodeler and ATP, i.e., no fractionation of the nonremodeled, remodeled, and slid particles was carried out in the past. We emphasize that we were only able to identify the remosome because of the use of a combination of very high-resolution microscopy techniques, specially built image analysis software, unique biochemical approaches, and appropriate nucleosomal templates.

1. Wu C, Travers A (2004) A "one-pot" assay for the accessibility of DNA in a nucleosome core particle. *Nucleic Acids Res* 32(15):e122.
2. Luger K, Rechsteiner TJ, Richmond TJ (1999) Expression and purification of recombinant histones and nucleosome reconstitution. *Methods Mol Biol* 119:1–16.
3. Cairns BR et al. (1996) RSC, an essential, abundant chromatin-remodeling complex. *Cell* 87(7):1249–1260.
4. Mutskov V et al. (1998) Persistent interactions of core histone tails with nucleosomal DNA following acetylation and transcription factor binding. *Mol Cell Biol* 18:6293–6304.
5. de la Barre AE, Angelov D, Molla A, Dimitrov S (2001) The N-terminus of histone H2B, but not that of histone H3 or its phosphorylation, is essential for chromosome condensation. *Embo J* 20(22):6383–6393.
6. Montel F, Fontaine E, St-Jean P, Castelnovo M, Faivre-Moskalenko C (2007) Atomic force microscopy imaging of SWI/SNF action: Mapping the nucleosome remodeling and sliding. *Biophys J* 93(2):566–578.
7. Dubochet J et al. (1988) Cryo-electron microscopy of vitrified specimens. *Q Rev Biophys* 21(2):129–228.
8. Saha A, Wittmeyer J, Cairns BR (2005) Chromatin remodeling through directional DNA translocation from an internal nucleosomal site. *Nat Struct Mol Biol* 12(9):747–755.
9. Zofall M, Persinger J, Kassabov SR, Bartholomew B (2006) Chromatin remodeling by ISW2 and SWI/SNF requires DNA translocation inside the nucleosome. *Nat Struct Mol Biol* 13(4):339–346.
10. Lia G et al. (2006) Direct observation of DNA distortion by the RSC complex. *Mol Cell* 21 (3):417–425.
11. Zhang Y et al. (2006) DNA translocation and loop formation mechanism of chromatin remodeling by SWI/SNF and RSC. *Mol Cell* 24(4):559–568.
12. Clapier CR, Cairns BR (2009) The biology of chromatin remodeling complexes. *Annu Rev Biochem* 78:273–304.
13. Kwon H, Imbalzano AN, Khavari PA, Kingston RE, Green MR (1994) Nucleosome disruption and enhancement of activator binding by a human SW1/SNF complex. *Nature* 370(6489):477–481.
14. Côté J, Peterson CL, Workman JL (1998) Perturbation of nucleosome core structure by the SWI/SNF complex persists after its detachement, enhancing subsequent transcription factor binding. *Proc Natl Acad Sci USA* 95:4947–4952.
15. Bruno M et al. (2003) Histone H2A/H2B dimer exchange by ATP-dependent chromatin remodeling activities. *Mol Cell* 12(6):1599–1606.

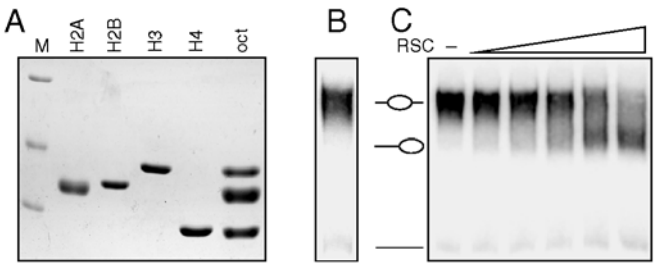

Fig. S1. The reconstituted nucleosomes are efficiently mobilized by RSC. (*A*) 18% SDS-PAGE of the recombinant histones used for reconstitution and the histone composition (oct) of the reconstituted particles. (*B*) Band shift assay of the reconstituted nucleosomes. Nucleosomes were reconstituted on a 255 bp 601 positioning sequence. Note that, under the conditions of reconstitution, no free DNA was observed. (*C*) RSC mobilization assay. Reconstituted nucleosomes were incubated with increasing amounts of RSC in the presence of ATP.

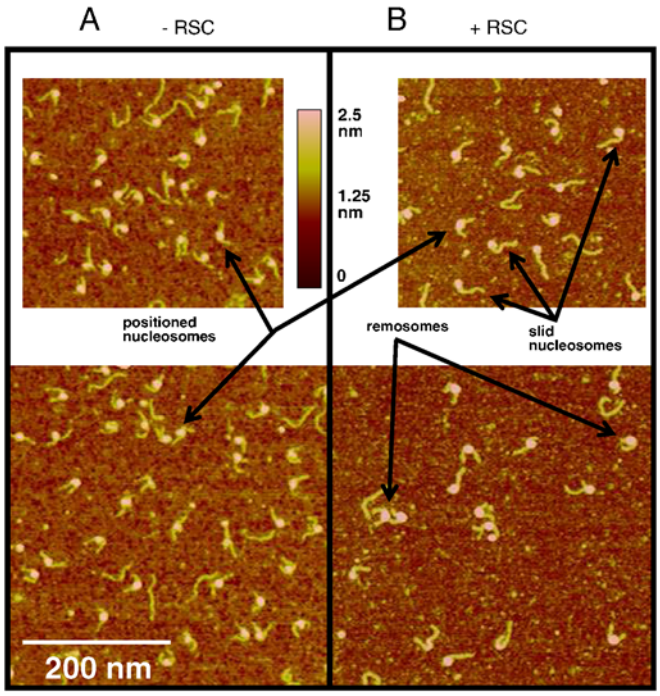

Fig. S2. Large field of tapping mode AFM images of mononucleosomes incubated with RSC. Mononucleosomes, reconstituted on a 255 bp 601 fragment, were incubated with RSC at 29 °C and in RB containing 10 mM Tris-HCl, pH 7.4, 2.5 mM $MgCl_2$, and 1 mM ATP. The reaction was stopped after 30 min by diluting 10 times in TE buffer (Tris-HCl 10 mM, pH 7.4, EDTA 1 mM) and 5 μLof the mix was deposited onto the functionalized APTES-mica surface for AFM imaging. (*A*) Control mononucleosomes in the absence of RSC. (*B*) Mononucleosomes incubated with RSC at 29 °C for 30 min. The three different states of the mononucleosomes are shown by arrows as indicated: middle positioned nucleosomes (unprocessed by RSC), end positioned (slid nucleosomes), and remosomes (overcomplexed particles).

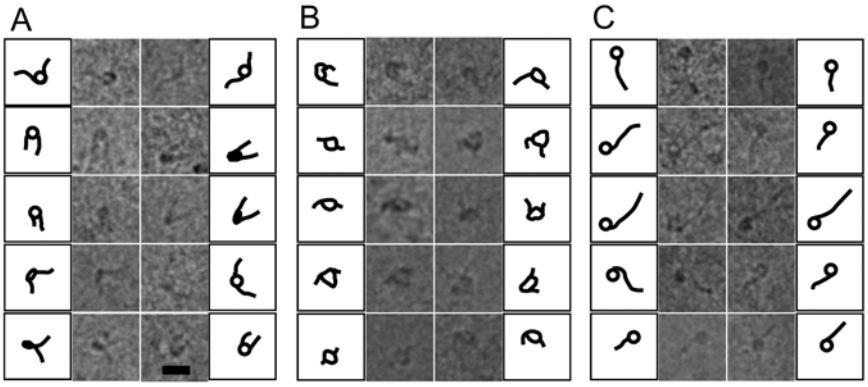

D

Nucleosome	DNA Complexed length (Lc) ± SEM	Position (ΔL/2) ± SEM
Unremodeled	149.1±1.3 bp	3.1±0.8 bp
Remosome	183.0±1.8 bp	6.3±0.9 bp
Slid	143.0±1.8 bp	56.0±1.8 bp

Fig. S3. Representative EC-M images of unremodeled (*A*), remosome (*B*), and slid (*C*) particles. Centrally positioned nucleosomes reconstituted on a 255 bp 601 DNA were treated with RSC, immediately vitrified, and visualized by EC-M. Each micrograph is accompanied by schematic drawing illustrating the shape of the DNA observed in the micrographs. (Scale bar, 25 nm). (*D*) Table showing the measurements of DNA-complexed length (L_c) and octamer position ($\Delta L/2$) for nucleosome species presented in Fig. 3*A*.

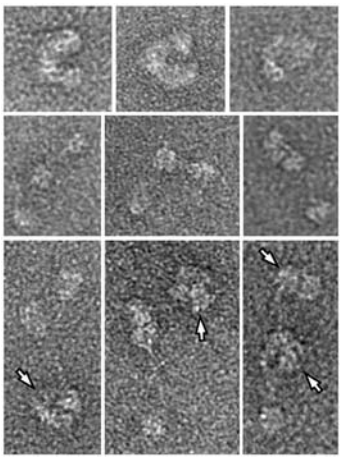

Fig. S4. The RSC complex is associated with a single nucleosome within a trinucleosome. To study the association with RSC with the trinucleosomes, H1-depleted trinucleosomes were isolated from chicken erythrocyte nuclei and complexed with RSC. They were then fixed with formaldehyde, negatively stained, and used for the EM experiments. Note that under the conditions used in the AFM and EC-M experiments, we were able to observe only very few RSC-nucleosome complexes, suggesting that once the remosomes are formed or the nucleosomes are mobilized, RSC dissociates from its substrate (Figs. 1–3). Fixation was thus required to visualize the RSC-nucleosome complex under our experimental conditions. The first and the second row show representative electron micrographs of RSC and trinucleosomes alone, respectively. On the third row are shown the RSC-trinucleosome complexes. The RSC alone showed the typical "crescent" shape conformation with a central cavity (first row), a result in agreement with the previous reports (8, 9). However, when RSC was allowed to associate with the trinucleosome, a much larger structure (white arrows) than a single nucleosome was observed (compare the structures of the trinucleosomes of the second row with these of the third row). The linker DNA connecting this large structure with the adjacent nucleosomes was clearly visible (third row). We attributed this structure to the RSC-single nucleosome complex (arrows). Interestingly, this large structure exhibited a uniform staining, demonstrating that the nucleosome indeed filled the RSC cavity (third row). This result is in agreement with the recent EC-M data showing that RSC forms a complex with a single isolated nucleosome (10) and further illustrates that this is also the case when nucleosomal arrays are used as substrate for the remodeler.

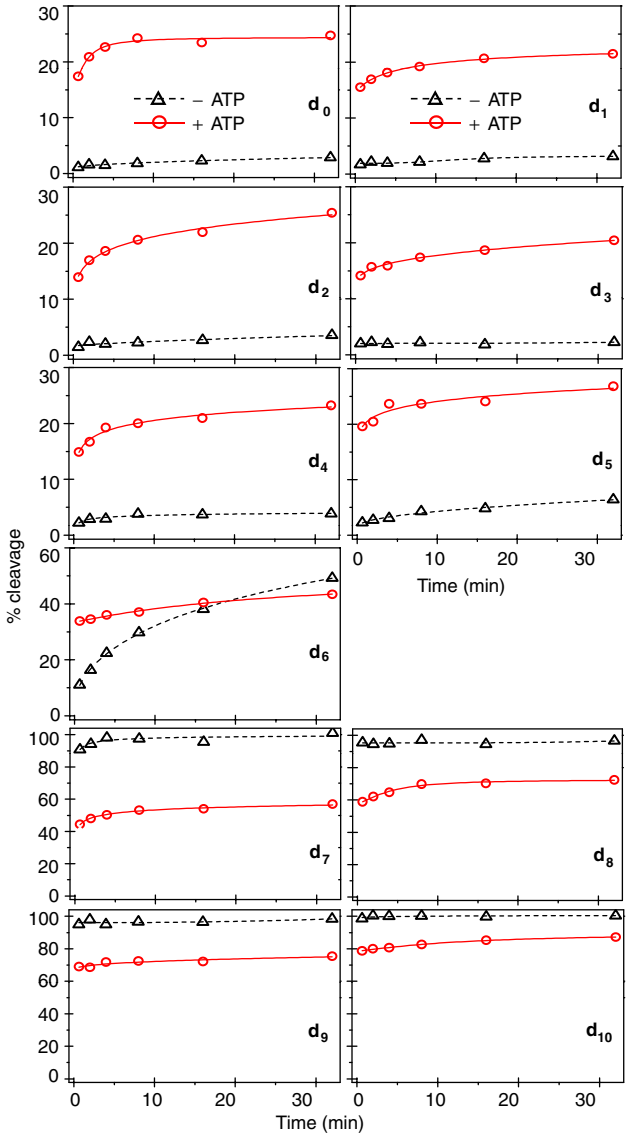

Fig. S5. Time course of *Hae*III acessibility of remosomes in solution. Eleven different ^{32}P-end labeled mutated 255 bp 601.2 DNA sequences were used to reconstitute centrally positioned nucleosomes (each one of the sequences bears a unique *Hae*III restriction site, designated dyad-0 (d_0) to dyad-10 (d_{10}), where the number indicates the number of helical turns from the dyad). An equimolar mixture of the 10 centrally positioned nucleosomes was incubated with RSC in the absence (–ATP) or presence of ATP (+ATP) in a way to produce about 50% of slid end-positioned nucleosomes. The reaction mixtures were then separated on a 5% PAGE under native conditions. Then the upper band (containing the nonslid particles) was excised from the gel and particles were eluted from the gel slices. The eluted samples were then digested with 2 units/μL of *Hae*III and the digested DNA run on 8% PAGE under denaturing conditions. After exposure of the dried gel, product bands from the experiment for each time point and for each dyad were quantified and expressed as percentage of cut fraction.

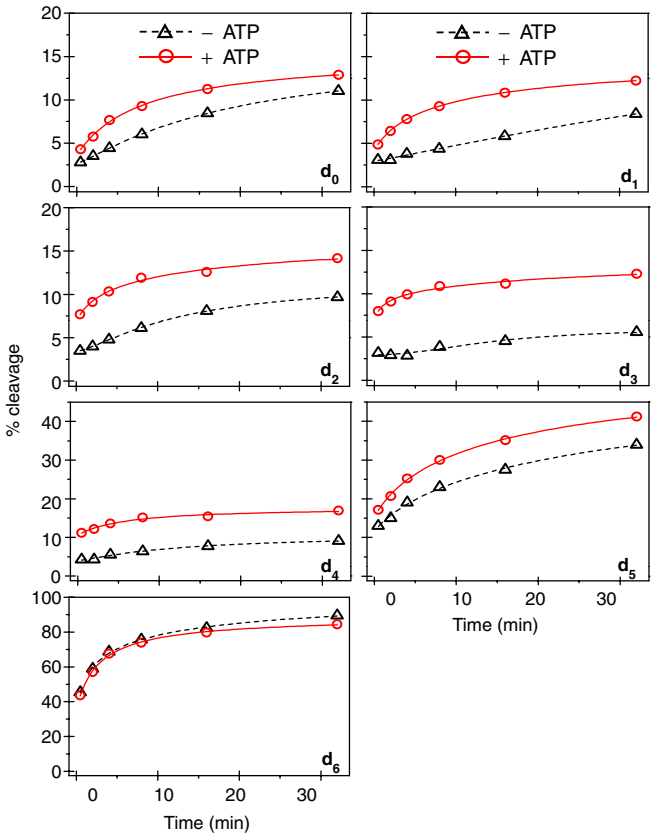

Fig. S6. Time course of the *Hae*III accessibility of RSC-treated core particles in solution. Eight different ^{32}P-end labeled mutated 147 bp 601.2 DNA sequences were used to reconstitute core particles (each one of the sequences bears a unique *Hae*III restriction site, designated dyad-0 (d_0) to dyad-7 (d_7), where the number indicated the number of helical turns from the dyad). The core particles were incubated with RSC for 30 min at 29 °C and, after arresting the remodeling reaction, they were digested with *Hae*III (5 U/μL) for the times indicated. The cleaved DNA was run on an 8% PAGE under denaturing conditions. After exposure of the dried gel, product bands from the experiment were quantified and expressed as percentage of cut fraction. Data for the time course of the accessibility toward *Hae*III of each dyad, with the exception of d_7 are presented.

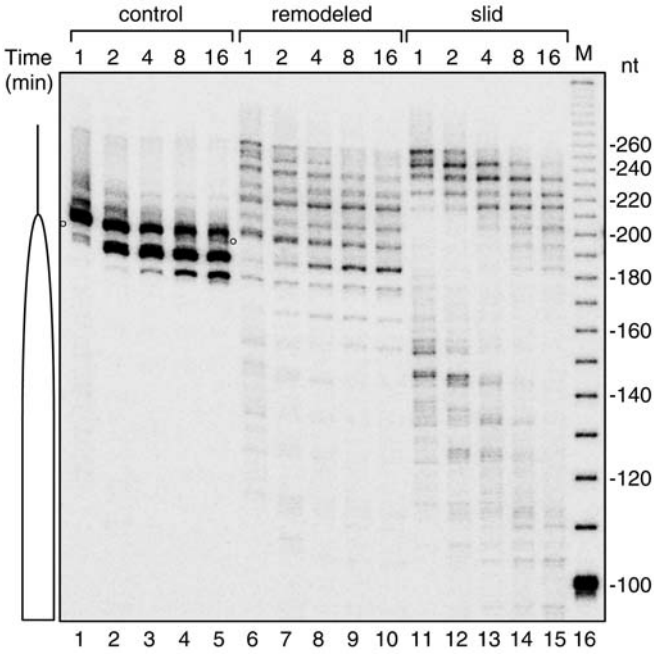

Fig. S7. Exonuclease III mapping. Centrally positioned nucleosomes were reconstituted on a 5′ ^{32}P-labeled 255 bp 601 DNA sequence and incubated with RSC either in the absence (control) or in the presence of ATP (in a way to produce about 50% of slid end-positioned nucleosomes). The reaction mixtures were then run on a 5% PAGE under native conditions, the bands corresponding to the control and the slid nucleosomes and the remosomes were excised from the gel and eluted. The gel eluted particles as well as naked 255 bp 601 DNA were next digested with Exo III for the indicated time points and the cleaved DNA was run on 8% PAGE under denaturing conditions. (M) DNA molecular mass markers; (o) indicates the nucleosome DNA border. Note the very different digestion pattern of the three types of particles. As expected, the control particle shows an Exo III digestion pattern, typical for the centrally positioned nucleosome with stops at 200 bp (the border of the nucleosome) and 190 bp (10 bp inside the nucleosome) positions (lanes 1–5). In contrast, the slid nucleosome digestion pattern exhibits several stops at both ends of the 255 bp fragment, separated by about 50–60 bp in length DNA sequence where no stops are observed (lanes 11–15). We attribute the stops to the digestion inside of the nucleosomes slid and relocated to both DNA ends. The 50–60 bp sequence would correspond to the noncovered by histones naked DNA common for both slid particles located at each end of the 255 bp DNA. Remarkably, the remosome fraction exhibits highly asymmetrical Exo III digestion profile, with stops observed essentially only at one end of the 255 bp fragment (lanes 6–10). We attribute these stops to reflect the presence of nonslid remosome structures with different (higher than 150 bp) length of overcomplexed DNA. [Note that the length of the remosomal DNA peaked at 180–190 bp, but the length distribution function is rather broad and such variations (corresponding to the stops in the Exo III digestion profile) in the overcomplexed length are expected to be observed, see Fig. 2 for detail.]

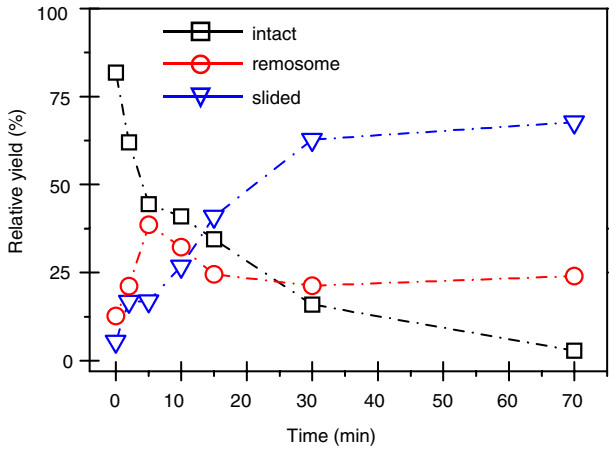

Fig. S8. AFM experiments show that the remosomes are intermediary particles generated during the RSC nucleosome mobilization reaction. Centrally positioned 601 nucleosomes were incubated with RSC in the presence of ATP and the reaction was stopped at the times indicated. Then the different species present in the reaction mixture were visualized by AFM. The amount of each individual type of particles was measured and after normalization, the percentage of intact nucleosomes, remosomes, and slid nucleosomes was presented as a function of the time of the remodeling reaction. Note that the initial increase of remosome amount is followed by a gradual decrease of the amount of this type of particles as the remodeling reaction proceeds.